

Structural Optimization of Internally Reinforced Beams Subjected to Uncoupled and Coupled Bending and Torsion Loadings for Industrial Applications

Hugo M. SILVA
Jose F. MEIRELES

University of Minho

*Department of Mechanical Engineering
Campus of Azurém, 4800-058 Guimarães, Portugal
hugolopessilva@gmail.com
meireles@dem.uminho.pt*

Received (29 January 2017)

Revised (6 March 2017)

Accepted (11 May 2017)

In this work, novel types of internally reinforced hollow-box beams were structurally optimized using a Finite Element Updating code built in MATLAB. In total, 24 different beams were optimized under uncoupled bending and torsion loads. A new objective function was defined in order to consider the balance between mass and deflection on relevant nodal points. New formulae were developed in order to assess the efficiency of the code and of the structures. The efficiency of the code is determined by comparing the Finite Element results of the optimized solutions using ANSYS with the initial solutions. It was concluded that the optimization algorithm, built in Sequential Quadratic Programming (SQP) allowed to improve the effective mechanical behavior under bending in 8500%, showing a much better behavior than under torsion loadings. Therefore, the developed algorithm is effective in optimizing the novel FEM models under the studied conditions.

Keywords: structural optimization, mechanical behavior, Finite Element Method, Solid Mechanics, MATLAB, ANSYS.

1. Introduction

In the last years, there has been an increase in the use of computers in engineering and applied sciences. This is due to the extreme improvement of the personal computers capabilities, which made possible to solve complex engineering problems from several hours to few days. The Finite Element Method-FEM programs, like ANSYS, are extremely powerful, especially when they are allied with optimization procedures. The FEM has some limitations in the results accuracy when modeling complex structures [1]; however, there have been many developments in this field.

For instance, X. Bin has modeled an aerial working vehicle with good correlation between results [2]. Several optimization methods have been developed over the last few years with application to structural static analysis [3–7]). S. Kalanta et al. shown that 2D optimization problems, namely in terms of mathematical models and solution algorithms, can be adopted for solutions of 3D optimization problems [8]). H. Silva and J. Meireles developed a Finite Element Model Updating methodology for static analysis, with the main aim to optimize the mechanical behavior of steel objects subjected to bending and torsion uncoupled loadings ([9]; [10]) Some authors applied optimization methods to beams of various cross-sections manufactured by cold forming in order to optimize relevant geometric variables of the structures [11]. A new global optimization approach that is well suited for the optimization of cross-sections is presented by H. Liu et al. in the paper "Knowledge-based global optimization of cold-formed steel columns". It is found that the developed optimization process can effectively learn from the optimization processes and apply the knowledge on related design optimization problems. This is an efficient learning mechanism that is not present in most optimization schemes [12]. E. Magnucka-Blandzi and K. Magnucki wrote a paper about cold-formed thin-walled channel beams with open or closed flanges [13]. Leng et. al demonstrated the application of formal optimization tools with the aim of maximizing the compressive strength of an open cold-formed steel cross section. In this work, the cross section shape is not limited by pre-determined elements (flanges, webs, stiffeners, etc.), as is commonly required to meet the necessity of conventional code-based procedures for design that employ simplified closed-form stability analysis [14]. The design optimization of oval hollow-box beams made of stainless steel was studied by M. Theofanous et. al. The authors studied the structural response of stainless steel oval hollow section under compression [15]. Structures made by several beams were studied by Lagaros et al. The authors performed an optimum design of 3D steel structures having perforated I-section beams [16]. Tsavdaridis and D'Mello studied the optimization of novel elliptically-based web opening Shapes. The work developed by the authors improves the structural behavior of perforated beams while aiming an economic design in terms of manufacture and usage [17]. McKinstry et al., studied the optimal design of fabricated steel beams for applications on long-span portal frames. The design optimization takes into account several relevant factors, such as ultimate and serviceability limit states, and deflection limits, as recommended by the Steel Construction Institute (SCI). The authors used a genetic algorithm (GA) in order to optimize geometric variables of the plates, which were used for columns, rafters and haunches [18]. Tran and Li presented a global optimization method for the design of the cross-section of channel beams under uniformly distributed transverse loading. The optimization presented by the authors is carried out using the trust-region method (TRM), and it was based on factors, such as the "...failure modes of yielding strength, deflection limitation, local buckling, distortional buckling and lateral-torsional buckling", Cited from [19]. In this paper, Finite Element models are optimized in static analysis by coupling MATLAB and ANSYS. This paper studies solutions already presented [20, 21].

2. Sequential Quadratic Programming (SQP)

SQP methods are robust methods in the field of nonlinear programming. For example, Schittkowski [22], has implemented and tested a version that performs better than every other tested method in terms of efficiency, accuracy, and percentage of successful solutions. The development was tested over a large number of test problems. Having as basis the work of Biggs [23], Han [24], and Powell ([25, 26]), this method permits the close mimic of the Newton's method in constrained optimization in the same manner as it is done for unconstrained optimization. It works by doing an approximation of the Hessian of the Lagrangian function using a quasi-Newton updating method at each major iteration, which is used after to generate a QP subproblem. The solution of this subproblem is then used to form a search direction for a line search procedure. An overview of SQP is found in Fletcher [27], Gill et al. [28], Powell [29], and Schittkowski [30]. The general method is described next. The main idea of the SQP is the formulation of a QP subproblem based on a quadratic approximation of the Lagrangian function, as shown the Eq. (1):

$$L(x, \lambda) = f(x) + \sum_{i=1}^m \lambda_i \cdot g_i(x) \quad (1)$$

A simplification of the Eq. 1 is done using the assumption that bound constraints have been expressed as inequality constraints. The QP subproblem is obtained by the linearization of the nonlinear constraints.

The Quadratic Problem (QP) can be described by the set of following equations:

$$\begin{aligned} \min \quad & \frac{1}{2} d^T H_k d + \nabla f(x_k)^T d \\ \nabla g_i(x_k)^T d + g_i(x_k) &= 0 \quad i = 1, \dots, m_e \\ \nabla g_i(x_k)^T d + g_i(x_k) &\leq 0 \quad i = m_e + 1, \dots, m \end{aligned} \quad (2)$$

The solution is then used to form a new iterate, shown in (3):

$$x_{k+1} = x_k + \alpha_k d_k \quad (3)$$

The parameter α_k is known as step length. Its determination happens by means of an appropriate line search procedure, in order for an enough decrease in a merit function to is obtained. The matrix H_k is a positive definite approximation of the Hessian matrix of the Lagrangian function, as shown in (1). A constrained problem can usually be solved in fewer iteration that an unconstrained problem in nonlinear optimization using SQP. The main reason for this fact, is that, the limits that are imposed in the constrained optimization problem is a useful information that allows the optimizer to find feasibility with more easiness, by directing the search and setting the step length more efficiently [31].

3. Active Set Algorithm

The optimization function used in the MATLAB programming code was `fmincon`. The `fmincon` function attempts to find the minimum of a constrained nonlinear

multivariable function is a Nonlinear programming solver. It searches for a minimum in a problem described by (4):

$$\min_x f(x) \text{ such that } \begin{cases} c(x) \leq 0 \\ ceq(x) = 0 \\ A \cdot x \leq b \\ Aeq \cdot x = beq \\ lb \leq x \leq ub \end{cases} \quad (4)$$

where: b and beq are vectors, A and Aeq are matrices, $c(x)$ and $ceq(x)$ are functions that return vectors, and $f(x)$ is a function that returns a scalar, $f(x)$, $c(x)$, and $ceq(x)$ can be nonlinear functions; x , lb , and ub can be passed as vectors or matrices [32].

In a constrained optimization problem, such as in this, the aim is usually to modify the problem, making it become a sub problem which requires less difficulty and which can be solved and used in an iterative process. Early methods used the translation of the constrained problem to a basic unconstrained problem. This was usually done by means of a penalty function for constraints that are near or beyond the constraint boundary. This ensure that the constrained problem is solved using several sequential parameterized unconstrained optimizations. These optimizations cause the sequence limit to converge to the constrained problem. These early methods are nowadays considered of low inefficiency, and therefore, obsolete. They have been replaced by newer methods that are focused on the solving of the Karush–Kuhn–Tucker (KKT) equations. The KKT equations are needed conditions to achieve optimality on a constrained optimization problem. The KKT equations are both needed and enough for a global solution point in the case of problems which belong to the convex programming problem class. To be considered as such, $f(x)$ and $G_i(x)$, $i = 1, m$, must be convex functions.

The KKT equations can be expressed as (5):

$$\begin{aligned} \nabla f(x^*) + \sum_{i=1}^m \lambda_i \cdot \nabla G_i(x^*) &= 0 \\ \lambda_i \cdot \nabla G_i(x^*) &= 0 \quad i = 1, \dots, m_e \\ \lambda_i &\geq 0, i = m_e + 1, \dots, m \end{aligned} \quad (5)$$

in addition to the original constraints (6):

$$\begin{aligned} g(x) &= 0 \\ h(x) &\leq 0 \\ xl &\leq x \leq xu \end{aligned} \quad (6)$$

where: x is the vector of the optimization parameters, $q(x)$, $g(x)$ and $h(x)$ are functions.

The first equation describes the canceling of the gradients between the objective function and the active constraints at the solution point. For this to happen, Lagrange multipliers (λ_i , $i = 1, m$) are needed for the balance of the deviations in the

same magnitude of the objective function and constraint gradients. Due to the fact that only active constraints are included in the canceling, inactive constraints must not be included in the operation, and, therefore, are given Lagrange multipliers equal to 0. This fact is stated in an implicit manner in the last two KKT equations. The solution of the KKT equations serve as the basis of various nonlinear programming algorithms, which attempt to compute the Lagrange multipliers directly. For instance, constrained quasi-Newton methods guarantee superlinear convergence by doing the accumulation of second-order information regarding the KKT equations using a quasi-Newton updating procedure. These methods are commonly known as Sequential Quadratic Programming (SQP) methods. A Quadratic Programming (QP) subproblem is solved at each major iteration. This solving method is also known as Iterative Quadratic Programming, Recursive Quadratic Programming, and Constrained Variable Metric [33].

4. Numerical Procedure

4.1. FEM models

In order to obtain an effective response to transversal beam deflection, in terms of stiffness, twelve Finite Element Method (FEM) models were built in the commercial FEM program ANSYS. These models represent the novel beams. The novel beams are composed by two sandwich panels on the top and on the bottom and a reinforcement pattern on the sides, as shown in the Fig. 1:

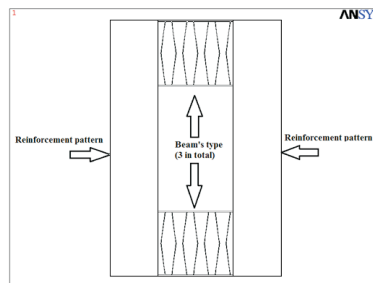


Figure 1 Configuration of beam types 20, 21

As shown in the Fig. 1, the construction technique involves concentric tubes of rectangular shape, that will be ribbed in its ends to maximize its stiffness capabilities (Fig. 1). This constructing is based on the principle that this type of beams needs a zone along which accessories pass, such as compressed air tubes and electric cables. The central zone of the beam was chosen because that zone contains the neutral axis. In the peripheral zone, there are two lateral zones, and two other zones: one at the top and the other at the bottom. In the two top and bottom zones, the reinforcement is fundamental to increase bending stiffness, while the lateral zones increase mainly the torsion stiffness. The chosen geometry for the upper and bottom reinforcing zones are shown in the Fig. 2. These geometries were previously studied in sandwich beams in [34, 35].

In the lateral zones, the geometries of the reinforcements designed to improve torsion stiffness are defined according to the Figs. 3 and 4.

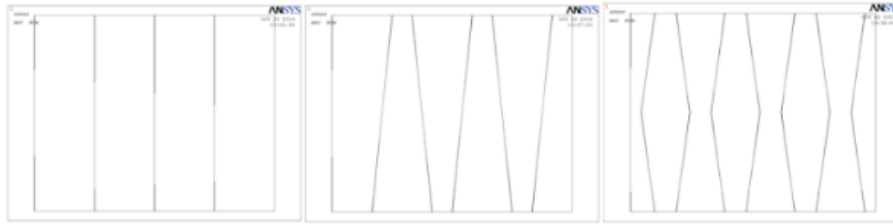


Figure 2 Section view of the sandwich beams: web-core (left) (beam 1), corrugated-core (middle) (beam 2) and honeycomb core (right) (beam 3)

The Figures 3 and 4 show the inner areas reinforcements of the novel beams:

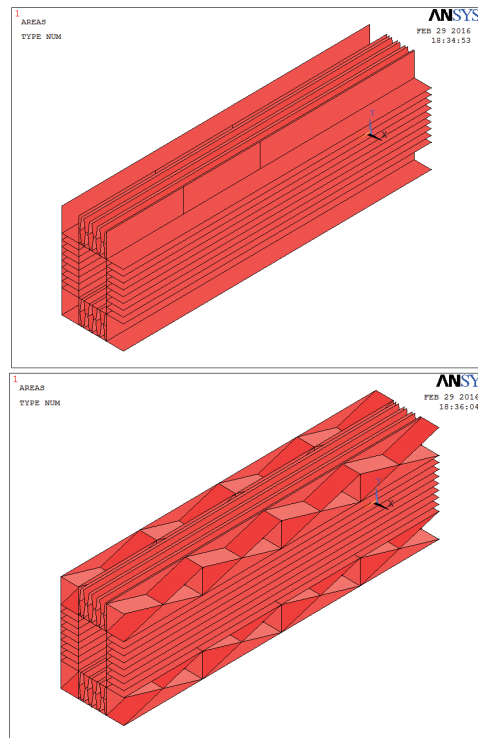


Figure 3 Areas of the FEM models of the beams: Pattern 1 (left) and Pattern 2 (right). The top and right side areas are totally hidden to allow inner view

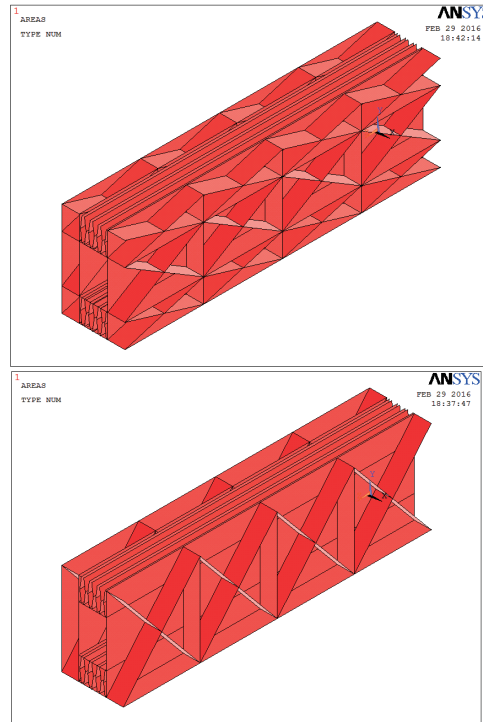


Figure 4 Areas of the FEM models of the beams: Pattern 3 (top) and Pattern 4 (bottom). The top and right side areas are totally hidden to allow inner view

The Fig. 5 shows an additional internal reinforcement on one of the beams, named transversal reinforcements. These transversal reinforcements are used in order to evaluate its influence on the improvement of the part's stiffness. In this work, the beams can be of two types: A and B. The beams A don't have the transversal reinforcements that are along the beam's flange, while all the beams B have them. The models of the Fig. 3 and 4 are of the A type, while the model represented on the Fig. 5 is of the B type.

The results obtained in this work are in relation to a simple hollow-box beam, designated by Hollow Solid section, and abbreviated HSS with similar dimensions, but with a thickness of 2 mm, and without the internal reinforcements, as shown in the Fig. 6.

The HSS beams (Fig. 6), were studied using the same conditions as on the sandwich beams. These conditions and geometries, originally presented by (Silva and Meireles 2015; Silva and Meireles -), may have their mechanical behavior improved by the use of optimization. For the FEM modelling, the used element was SHELL63 (Shell Elastic 4 nodes). The elements are free quadrilateral elements with a mean length of 0,0025 m. A mesh sensitivity analysis on the exact same geometries was already done by [20, 21].

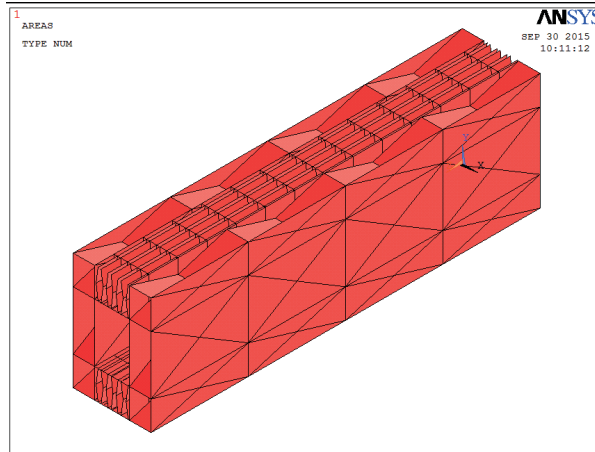


Figure 5 Internal reinforcements on beam 3 pattern 3 [20, 21]

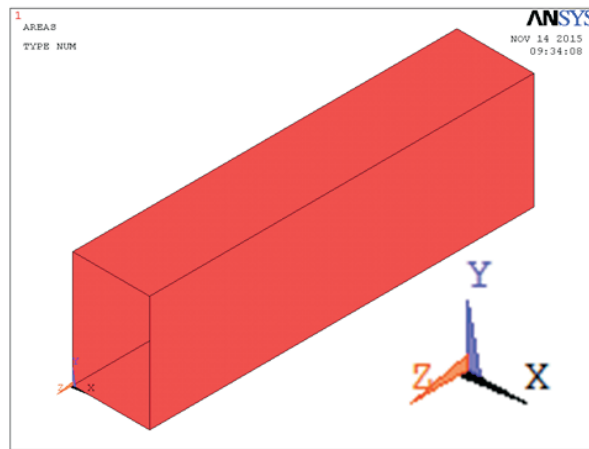


Figure 6 Areas of the FEM model representing the HSS or simple beam

The beam was constrained in the lines of the extremities ($z = 0$ and $z = 1$), being the support type simply supported at its ends, as shown in Fig. 7. Concentrated loads were used by simplification in order to simulate the action of bending and torsion. Bending was applied by one concentrated load of 1500 N, on the center of the top face, as shown in the Fig. 7 (top). Torsion is applied by means of a binary load of 2000 N, as in Fig. 7 (bottom). The same load intensities were already applied to similar models by [20, 21].

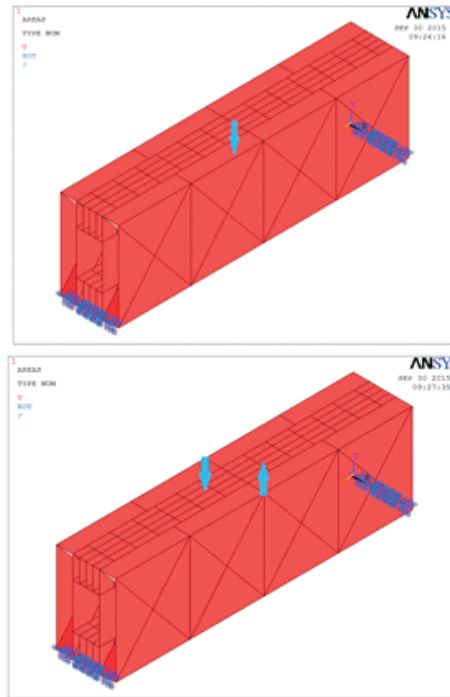


Figure 7 DOF Constraints and loadings in bending (top) and torsion (bottom) [20, 21]

4.2. Optimization

For the optimization process, the models were optimized in terms of nodal displacements in the y direction, measured on the three points, as shown in the Fig. 8, and total mass of the model. According to Newton's 2nd law, the force that the beam is subjected to is very closely related to the mass. The beam's mass can be reduced using materials having low density, however, these materials reduce the Elasticity Modulus significantly, The composite solutions, such as carbon fiber, are good in terms of Young's Modulus, but are not widely accepted due to their high cost. Due to this, the Young's Modulus is limited to the steel's. In contrast, the deflection in bending is inversely proportional to the Inertia Moment. For this reason, the search for sections with simultaneously high Inertia Moments and low mass is a challenge of this work.

In order to gather the displacements on the same points in each iteration, the ANSYS input file has instructions in order to collect the displacements on the nodes that are attached to the keypoints shown in the Fig. 8 (one by each keypoint). The keypoints are located on the edges (2) and on the center (1). These keypoints were chosen because their coordinate does not change during the optimization with the change in the variable values. These points are strongly reinforced with ribs, and, as such, it is not expected the local deformation to be significant for the considered thicknesses.

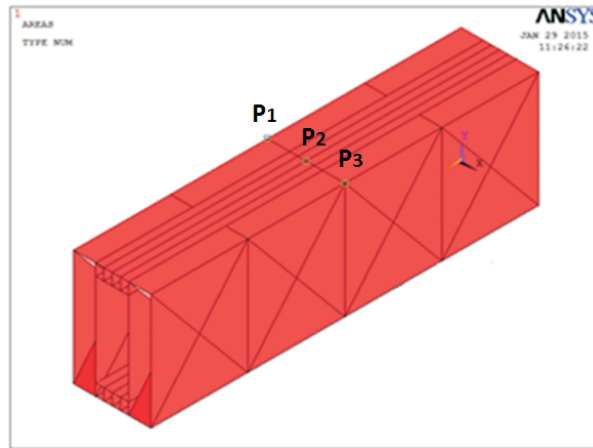


Figure 8 Points used to calculate displacements on optimization procedure

These points were chosen in places in which all coordinates are kept the same, in spite of the variation in the geometric variables. This avoids the direct influence of the change in the design variables on the results.

The methodology of the Finite Element Model Updating program developed in MATLAB in this work was previously developed for structural dynamic analysis by [1]. It was also adopted by [10] on structural static analysis. The Fig. 9 shows the interaction between ANSYS and the MATLAB optimization program.

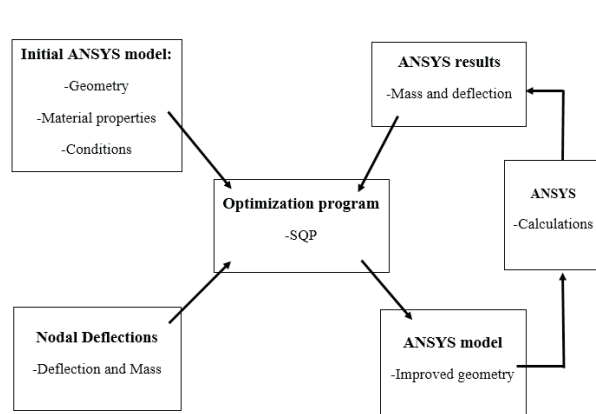


Figure 9 Functional flow chart of the optimization methodology [1]

In this methodology, the MATLAB program works together with ANSYS. According to ([10]): MATLAB controls the optimization by means of the MATLAB code and ANSYS calculates the FEM results. The objective function $q(x)$ used in this work is new, and the involved variables are also new (Fig. 10).

For the optimization, three design variables were chosen:

$LG1$: Half of the length of the x dimension of the inner beam,

$LG2$: Half of the length of the y dimension of the inner beam,

$LG3$: Thickness of the object.

Fig. 10 shows the geometric variables $LG1$, $LG2$ and $LG3$ on the beam 1 – pattern 1.

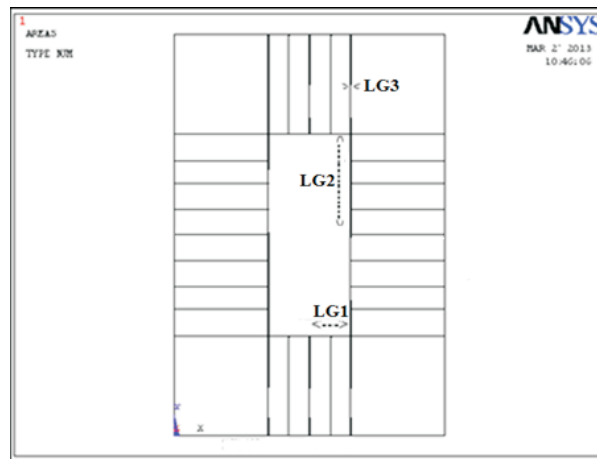


Figure 10 Geometric variables of the FEM model used on the design optimization

The outer section dimensions are kept, by principle, unaltered.

It is assumed that, from an industrial point of view, the whole beams shall be constructed with sheet of the same thickness. The aim is to obtain a set of reinforcements that is industrially easy to assemble.

4.3. The objective function

In relation to the code previously developed, a new objective function was developed. As the aim of this work is to obtain light and stiff structures, 2 terms must be included in the function: A mass term and a deflection term:

$$O(m, \delta) = f(m) + f(\delta) \quad (7)$$

where:

$O(m)$ is the objective function,

$f(m)$ is a function of the mass,

$f(\delta)$ is a function of the deflection.

As weights must also be included, in order to give more or less importance to each one of those terms, Eq. becomes:

$$O(m, \delta) = W_1 f(m) + W_2 f(\delta) \quad (8)$$

where:

W_1 is the weight relative to the mass,

W_2 is the weight relative to the deflection.

In this work $W_1 = W_2 = 0.5$.

The expression of $f(m)$ is given by the ratio of the sum of the element masses of the model being optimized and of the sum of the element masses of the initial model:

$$f(m) = \frac{\sum_{j=1}^n M_j}{\sum_{j=1}^n M_j^i} \quad (9)$$

where:

M_j is the element mass obtained in each nodal point and in each iteration,

M_j^i is the element mass obtained in each nodal point in the initial model.

The same logic also applies to the term $f(\delta)$:

$$f(\delta) = \frac{\sum_{j=1}^n |\delta_j|}{\sum_{j=1}^n |\delta_j^i|} \quad (10)$$

where:

δ_j is the nodal deflection obtained in each nodal point and in each iteration,

δ_j^i is the nodal deflection obtained in each nodal point in the initial model.

The absolute value of the deflections are sum because in torsion, the deflections on the points located at the edges are of opposite direction. What is important is the sum of those effects. In bending the absolute value has no influence on the results, because the deflections in all points have the same direction. However, for a question of coherence, the absolute value was also applied.

The ratio ensures that the objective function complies with the fmincon function in terms of function minimization. In fact, when the mass or deflection of the model being optimized decreases in relation to the initial model, the objective function also decreases, going towards the aim of objective function minimization. Substituting Eq. (3) and (4) on Eq. (2), it comes:

$$O(m, \delta) = W_1 \frac{\sum_{j=1}^n M_j}{\sum_{j=1}^n M_j^i} + W_2 \frac{\sum_{j=1}^n |\delta_j|}{\sum_{j=1}^n |\delta_j^i|} \quad (11)$$

This objective function was implemented in the MATLAB code.

5. Results

5.1. Optimization results

In order to improve the mechanical behavior of the studied models, optimization processes were used. These optimization processes use the objective function defined by (11), according to the aims of the project. In this optimization process, the basis

is an initial model with the same values of LG1, LG2 and LG3, as shown in the fig. 10. The FEM results of the initial and optimized models are compared with the HSS beam. The aim of the optimization routine is to minimize the objective function, to be a positive real number the closest possible to 0. The objective function value starts in 1 in every case, due to the fact that on the first iteration, the current model is the same as the initial model.

5.1.1. Bending

In the Fig. 11 one can see the final objective function value, obtained in the optimization routines for all beams, using (11) under bending loadings:

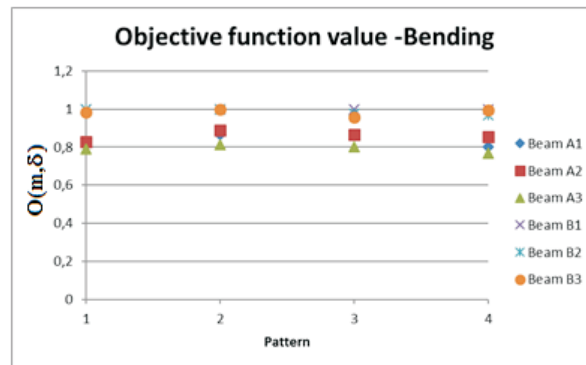


Figure 11 Final values of the objective function under bending loads

As it can be observed, in the models A1, pattern 1 and B2, pattern 1, the optimization was not able to get any improvement. This is due to the fact that any variation in the deflection term has a similar variation in the mass, but in opposite way. The final objective function value, along with the final variables values, of the variables already presented in the fig. 10, is shown in the table 1 for bending loadings.

5.1.2. Torsion

In the Fig. 12 one can see the final objective function value, obtained in the optimization routines for all beams.

The models A3 and B3 are the models that show the best results: an improvement of near 20%. These values were obtained by the application of (??) using the optimized and initial models, and were calculated numerically via MATLAB. The final objective function value, along with the final variables values, of the variables already presented in the Fig. 10, is shown in the Tab. 2 for torsion loadings.

Table 1 Final variable and objective function values obtained on the optimized models for bending loadings

Bending	A1	A2	A3	B1	B2	B3
Pattern 1						
PRLG1f	4.86	1.80	1.80	4.46	4.51	4.09
PRLG2f	7.73	9.26	8.32	7.53	7.52	7.46
PRLG3f	3.74	2.79	2.63	2.94	3.03	3.04
Final objective	0.98	0.83	0.79	1.00	1.00	0.98
Pattern 2						
PRLG1f	1.80	2.17	1.80	4.50	4.50	4.57
PRLG2f	10.15	7.61	11.90	7.49	7.49	7.52
PRLG3f	2.79	2.99	2.65	3.14	3.14	3.15
Final objective	0.87	0.89	0.81	1.00	1.00	1.00
Pattern 3						
PRLG1f	4.50	2.17	1.80	4.50	3.47	2.85
PRLG2f	7.51	9.02	9.52	7.58	8.20	8.84
PRLG3f	3.61	2.76	2.58	3.15	3.30	3.05
Final objective	0.97	0.86	0.80	1.00	0.98	0.96
Pattern 4						
PRLG1f	1.80	2.17	1.80	4.48	3.95	4.50
PRLG2f	8.05	7.70	8.36	7.56	9.19	7.55
PRLG3f	2.75	3.55	2.76	3.17	3.14	3.26
Final objective	0.80	0.85	0.77	1.00	0.97	1.00

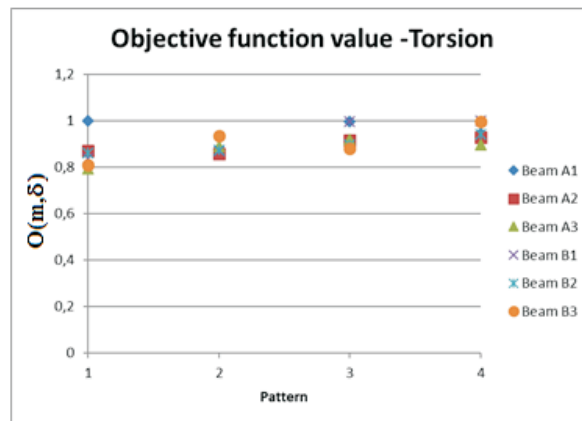
**Figure 12** Final values of the objective function under torsion loads

Table 2 Final variable and objective function values obtained on the optimized models for torsion loadings

Torsion	A1	A2	A3	B1	B2	B3
Pattern 1						
PRLG1f	4.54	6.95	7.20	7.20	7.20	7.20
PRLG2f	7.51	12.00	12.00	11.41	8.36	12.00
PRLG3f	3.01	3.36	3.50	3.34	3.18	2.38
Final objective	1.00	0.87	0.79	0.84	0.86	0.81
Pattern 2						
PRLG1f	7.20	7.20	7.20	7.20	7.20	7.20
PRLG2f	6.95	3.00	7.25	6.86	6.34	7.81
PRLG3f	3.47	3.34	3.29	3.26	3.13	1.54
Final objective	0.88	0.86	0.89	0.87	0.87	0.93
Pattern 3						
PRLG1f	4.50	7.20	7.20	4.50	7.20	7.20
PRLG2f	7.62	8.45	8.44	7.38	10.60	12.00
PRLG3f	3.24	4.05	3.34	3.23	3.42	3.71
Final objective	0.99	0.92	0.92	1.00	0.90	0.88
Pattern 4						
PRLG1f	4.28	6.22	3.42	4.50	4.49	4.78
PRLG2f	12.00	12.00	12.00	7.55	12.00	7.71
PRLG3f	3.42	3.71	3.61	3.16	3.62	3.22
Final objective	0.95	0.93	0.90	1.00	0.94	0.99

5.2. ANSYS results

In order to assess the effectiveness of the code and of the optimized models, the initial and the optimized models were run on ANSYS to collect FEM results. The difference between the initial and final models are the design variable values, modified by the optimization program. The mass is also affected with those changes. Mass and displacements in the y direction were collected in the FEM software ANSYS for bending loadings and mass, displacements in the y direction and twist angle (rotation around the z axis) were collected for torsion loads. Results for both the initial and optimized models are presented.

5.2.1. Relative Results: Comparison with a simple hollow-box beam

5.2.1.1. Factors Analyzed

The effectiveness of both initial models was assessed by the comparison of the effective mechanical behavior with a reference model, which is the HSS beam (Fig. 3), by means of analytic formulae. In bending, deflections were studied, while in torsion, both deflections and twist angle were studied. Parameters which quantify the effectiveness under bending and torsion combined loadings are also presented, for both initial and final models, being (18) and (19). The presented formulae are shown in the Tab. 3.

Table 3 Relative results: Comparison with HSS. *B* is the abbreviation for bending loadings, and *T* is the abbreviation for torsion loadings

Equation/loadings	B	T
$Imp_{\delta * m_i} (\%) = \frac{[a(\delta y) * m]_{HSS} - [a(\delta y) * m]_i}{[a(\delta y) * m]_i} * 100\%$ (14)	Yes	Yes
$Imp_{\delta * m_f} (\%) = \frac{[a(\delta y) * m]_{HSS} - [a(\delta y) * m]_f}{[a(\delta y) * m]_f} * 100\%$ (15)	Yes	Yes
$Imp_{\theta * m_i} (\%) = \frac{[a(\theta) * m]_{HSS} - [a(\theta) * m]_i}{[a(\theta) * m]_i} * 100\%$ (16)	No	Yes
$Imp_{\theta * m_f} (\%) = \frac{[a(\theta) * m]_{HSS} - [a(\theta) * m]_f}{[a(\theta) * m]_f} * 100\%$ (17)	No	Yes
$Imp_{\delta * m_i total} (\%) = \left[\left(\frac{[a(\delta y) * m]_{HSS} - [a(\delta y) * m]_i}{[a(\delta y) * m]_i} \right)_{bend} + \left(\frac{[a(\delta y) * m]_{HSS} - [a(\delta y) * m]_i}{[a(\delta y) * m]_i} \right)_{tors} \right]$ (18)	Yes	
$Imp_{\delta * m_f total} (\%) = \left[\left(\frac{[a(\delta y) * m]_{HSS} - [a(\delta y) * m]_f}{[a(\delta y) * m]_f} \right)_{bend} + \left(\frac{[a(\delta y) * m]_{HSS} - [a(\delta y) * m]_f}{[a(\delta y) * m]_f} \right)_{tors} \right]$ (19)	Yes	

where:

$[a(\delta y) * m]_{HSS}$ is the global maximum y deflection as measured on the two points multiplied by the total mass of the model for the reference model (HSS),

$[a(\delta y) * m]_i$ is the global maximum y deflection as measured on the two points multiplied by the total mass of the model for the initial models,

$[a(\delta y) * m]_f$ is the global maximum y deflection as measured on the two points multiplied by the total mass of the model for the final models,

$[a(\theta) * m]_{HSS}$ is the global maximum twist angle as measured on the two points multiplied by the total mass of the model for the reference model (HSS),

$[a(\theta) * m]_i$ is the global maximum twist angle as measured on the two points multiplied by the total mass of the model for the initial models,

$[a(\theta) * m]_f$ is the global maximum twist angle as measured on the two points multiplied by the total mass of the model for the final models.

5.2.1.2. Results Analysis

In order to compare the relative effectiveness of the solutions with the ultimate aim to reach the best solution, the formulae of the table 3 were applied analytically to the results collected from the models in ANSYS. In the Fig. 13, one can see the effective mechanical behavior results under bending loadings in comparison with a model of reference for all beams using (14).

According to the results shown in the Fig. 13, one can see that the best models are the models B1, B2 and B3 having the pattern 4, with improvements ranging from 7000% to near 8500%. There is an improvement for all models, although the model B1, pattern 4 shows the best results, showing an improvement of near 8500%. The worst models are the models A1, A2 and A3, which are worse than any of the B beams for every pattern.

In the Fig. 14, one can see the effective mechanical behavior of the optimized models in comparison with the simple hollow-box beam under bending loadings

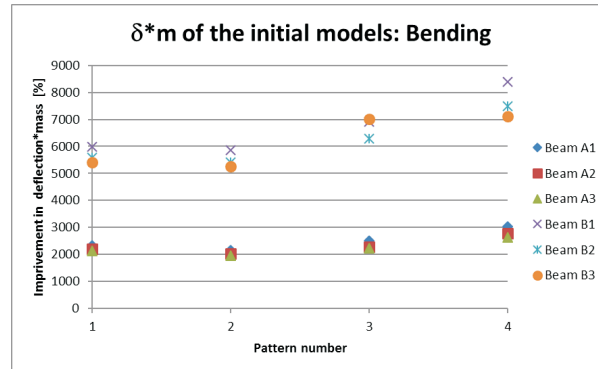


Figure 13 Effective mechanical behavior of the initial models in comparison with the simple hollow-box beam under bending loadings for beams without transversal reinforcements

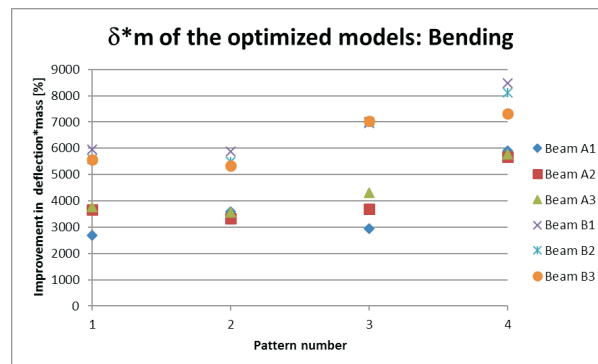


Figure 14 Effective mechanical behavior of the optimized models in comparison with the simple hollow-box beam under bending loadings for beams without transversal reinforcements

According to the results shown in the Fig. 14, one can see that the best models are the B models having the pattern 4, with improvements ranging from 7000% to 8500%. The A beams show an improvement of near 6000%. According to the fig. 14, the best models are the models of the pattern 4 with improvements ranging from 7000% to near 8500%, approximately. For both A and B models, there is an improvement for all models.

In the fig. 15, one can see the effective mechanical behavior results under torsion loadings in comparison with a model of reference for all beams, using (??).

According to the results shown in the Ffig. 15, there is a worsening for all models, although the pattern 4 shows the best results for all beams in comparison with the other patterns. The worst models are all the models of the pattern 1, with an improvement ranging from -70% to -60%. The beam B1 shows the best results

for every pattern. The best model is the Beam B1 pattern 4, with an improvement of -10%.

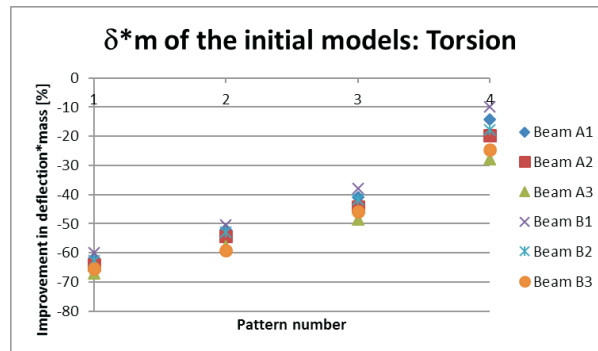


Figure 15 Effective mechanical behavior of the initial models in comparison with the simple hollow-box beam under torsion loadings for beams without transversal reinforcements

In the Fig. 16, one can see the effective mechanical behavior results under torsion loadings in comparison with a model of reference for beams without transversal reinforcements, using (15):

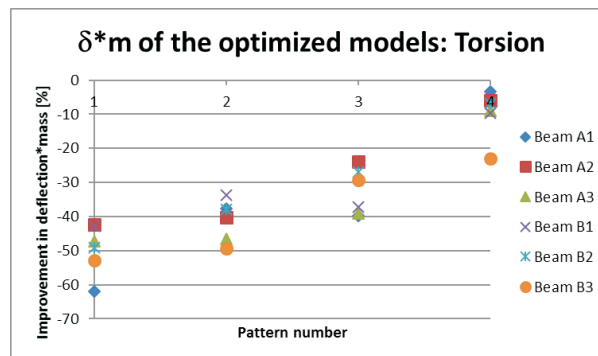


Figure 16 Effective mechanical behavior of the optimized models in comparison with the simple hollow-box beam under torsion loadings for beams without transversal reinforcements

According to the results shown in the Fig. 16, there is a worsening of the effective mechanical behavior for all the initial novel beams compared with simple hollow-box beams. One can see that the best models are the models of the pattern 4 with improvements ranging from -20% to near 0, approximately. The worst model is the models A1, pattern 1, for which there is an improvement of -60%. In the Fig. 17 one can see the effective mechanical behavior results under torsion loadings in terms of the twist angle in comparison with a model of reference, using (16):

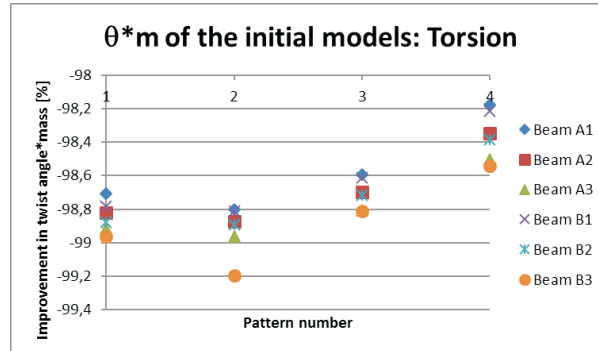


Figure 17 Effective mechanical behavior of the initial models in terms of the twist angle in comparison with the simple hollow-box beam under torsion loadings for beams without transversal reinforcements

According to the results shown in the Fig. 17, one can see that the best models are the models of the pattern 4 with improvements ranging from -98.5% to near -98.2, approximately. The beam A1 is the best for every pattern, followed by the beam B1. There is a worsening for all models without transversal reinforcements in terms of the effective twist angle. In the Fig. 18 one can see the effective mechanical behavior results under torsion loadings in terms of the twist angle in comparison with a model of reference, using (17), respectively.

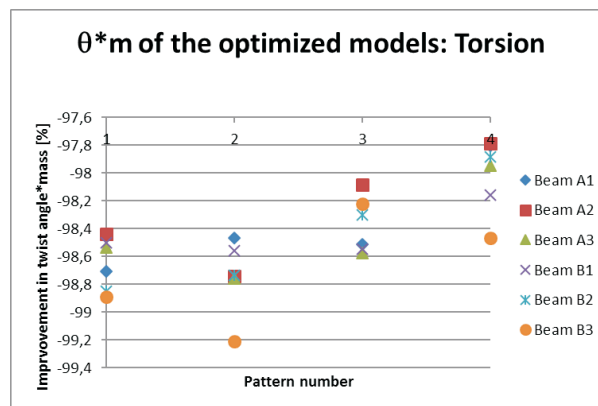


Figure 18 Effective mechanical behavior of the optimized models in terms of the twist angle in comparison with the simple hollow-box beam under torsion loadings for beams without transversal reinforcements

According to the results shown in the Fig. 18, there is a worsening for all models without transversal reinforcements in terms of the effective twist angle. One can

see that the best models are the models of the pattern 4 with improvements ranging from near -98.4% to near -97.8, approximately. Of those models, one can see that the best model is the Beam A2 pattern 4 with a worsening of -97.8%, approximately.

In the Fig. 19, one can see the effective mechanical behavior results in terms of total improvement in comparison with a model of reference, using (??).

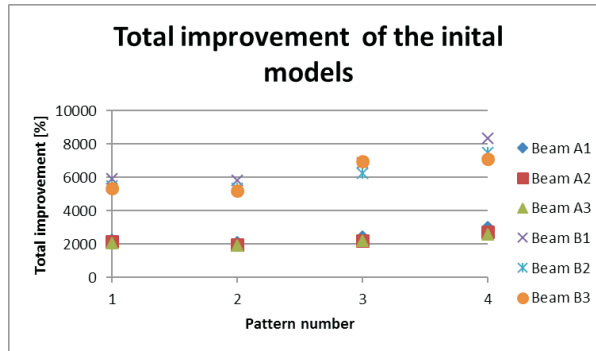


Figure 19 Total improvement of the initial models in terms of deflection in comparison with the simple hollow-box beam considering both bending and torsion loadings for beams without transversal reinforcements

According to the Fig. 19, the best models are the B models of the pattern 4 with improvements ranging from 7000% to near 8000%, approximately. One can see that the B models are better than the A models for every pattern. The results for the A beams vary from between near 2000% for every A beam, for the patterns 1,2 and 3, to near 3000% for the pattern 4. In the fig. 23, one can see the effective mechanical behavior results in terms of total improvement in comparison with a model of reference, using (19), respectively.

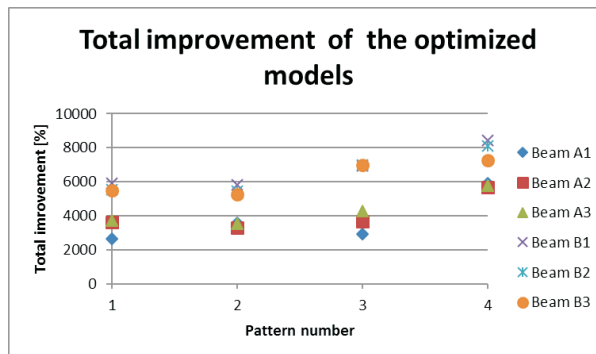


Figure 20 Total improvement of the optimized models in terms of deflection in comparison with the simple hollow-box beam considering both bending and torsion loadings for beams without transversal reinforcements

According to the Fig. 20, the best models are the B models of the pattern 4 with improvements ranging from 7000% to near 8000%, approximately. For all patterns, the B beams perform better than the A beams.

6. Results discussion

The results obtained under bending loadings prove that the developed beams are very effective under bending loadings. In fact, the sandwich reinforcements at the top and at the bottom dramatically increase the resistance moment and the inertia moment, while keeping the mass to a minimum. Under torsion loadings, the beams do not perform so well under the developed parameters due to the fact that the highest reinforcement density is located at the top and at the bottom. The reinforcement on the sides are more important for torsion, due to the fact that they are oriented transversally and diagonally, and, therefore, have an influence on the inertia moment under torsion loadings. The optimization procedure is shown to be very effective in optimizing most of the models, improving its effective mechanical behavior, both in bending and torsion loadings. The developed parameters (Tab. 3) allowed to evaluate the effectiveness of the optimization code and of the objective function, and also the evaluation of the effectiveness of the mechanical behavior of both initial and optimized models in terms of the Finite Element Method results obtained in ANSYS MECHANICAL APDL. The developed beams are very interesting for applications where bending loadings act isolate or coupled with torsion, in the case that the torsional component of the loadings have a less important effect than the bending component.

7. Conclusions

The following conclusions can be drawn from this work:

- The objective function developed is effective in improving the mechanical behavior of the FEM models while keeping the mass to a minimum both in torsion and in bending loadings. This can be proved by the results comparison between initial and optimized models.
- The models with transversal ribs are shown to be quite more effective than the ones without in terms of the total improvement.
- The best beam without transversal reinforcements after optimization is the Beam A1, pattern 4, with improvement close to 8500%.
- The best beam with transversal reinforcements is also the beam 1, Pattern 4.
- The novel beams are very effective in bending, while not so much under torsion loadings. The behavior under torsion loadings may be in reality better than in this study, due to the fact that one is comparing results on the point of loading application and that loading point is weaker in the novel beams than in the simple beams. For distributed loads, as it may happen in reality, it is expected that the load distribution will reduce the effect of the concentrated load.
- The studied beams can, therefore, be interesting for industrial applications, mainly in applications with mobile parts, where there is the need of light and stiff beams.

References

- [1] **De Meireles, J. F.:** Análise dinâmica de estruturas por modelos de elementos finitos identificados experimentalmente. PhD Thesis, University of Minho, **2007**.
- [2] **Bin, X., Nan, C. and Huajun, C.:** An integrated method of multi-objective optimization for complex mechanical structure, *Advances in Engineering Software* 41, 277–285, **2010**.
- [3] **Brill, E. D., Chang, S-Y and Hopkins, L. D.:** Modeling to generate alternatives: The HSJ approach and an illustration using a problem in land use planning. *Manage Sci*, 28:221, **1982**.
- [4] **Brill, E. D., Flach, J.M., Hopkins, L. D. and Ranjithan, S.:** MGA: A decision support system for complex, incompletely defined problems. *IEEE Trans Syst Man Cybern*, 20:745, **1990**.
- [5] **Baugh, J. W., Caldwell, S. and Brill, E. D.:** A mathematical programming approach for generating alternatives in discrete structural optimization, *Eng Optim*, 28:1, **1997**.
- [6] **Zárate, B.A., Caicedo, J.M.:** Finite element model updating: Multiple alternatives. Elsevier, *Engineering Structures*, 30, 3724–3730, **2008**.
- [7] **Bakir, P. G., Reynders, E., and De Roeck, G.:** An improved finite element model updating method by the global optimization technique Coupled Local Minimizers, *Computers and Structures*, 86, 1339–1352, **2008**.
- [8] **Kalanta, S., Atkociunas, J. and Venskus, A.:** Discrete optimization problems of the steel bar structures. *Engineering Structures*, 31, 1298–1304, **2009**.
- [9] **Silva, H. M., De Meireles, J. F.:** Determination of the Material/Geometry of the section most adequate for a static loaded beam subjected to a combination of bending and torsion. *Materials Science Forum* 730-732, 507–512, **2013**.
- [10] **Silva, H. M.:** Determination of the Material/Geometry of the section most adequate for a static loaded beam subjected to a combination of bending and torsion. MSc Thesis, University of Minho, **2011**.
- [11] **Lee, J., Kim, S-M, Park, H-S and Woo, B-H.:** Optimum design of cold-formed steel channel beams using micro Genetic Algorithm, *Engineering Structures*, 27, 17–24, **2005**.
- [12] **Liu, H., Igusa, T. and Schafer, B.W.:** Knowledge-based global optimization of cold-formed steel columns, *Thin-Walled Structures*, 42, 785–801, **2004**.
- [13] **Magnucka-blandzi, E., Magnucki, K.:** Buckling and optimal design of cold-formed thin-walled beams: Review of selected problems, *Thin-Walled Structures*, 49, 554–561, **2011**.
- [14] **Leng, J., Guest, J.K. and Schafer, B.W.:** Shape optimization of cold-formed steel columns, *Thin-Walled Structures*, 49, 1492–1503, **2011**.
- [15] **Theofanous, M., Chan, T.M. and Gardner, L.:** Structural response of stainless steel oval hollow section compression members, *Engineering Structures*, 31, 922–934, **2009**.
- [16] **Lagaros, N.D., Psarras, L.D., Papadrakakis, M. and Panagiotou, G.:** Optimum design of steel structures with web openings, *Engineering Structures*, 30, 2528–2537, **2008**.
- [17] **Tsavidaridis, K.D. and D’Mello, C.:** Optimisation of novel elliptically-based web opening shapes of perforated steel beams, *Journal of Constructional Steel Research*, 76, 39–53, **2012**.

- [18] **McKinstry, R., Lim, J.B.P., Tanyimboh, T.T., Phan D.T. and Sha, W.:** Optimal design of long-span steel portal frames using fabricated beams, *Journal of Constructional Steel Research*, 104, 104–114, **2015**.
- [19] **Tran, T., Li, L-Y.:** Global optimization of cold-formed steel channel sections. *Thin-Walled Structures*, 44, 399–406, **2006**.
- [20] **Silva, H. M., De Meireles, J. F.:** Feasibility of internally reinforced thin-walled beams for industrial applications, *Applied Mechanics and Materials*, 775, 119–124, **2015**.
- [21] **Silva, H. M., De Meireles, J. F.:** - Feasibility of Internally Stiffened Thin-Walled Beams for Industrial Applications [submitted].
- [22] **Schittkowski, K.:** NLQPL: A FORTRAN-Subroutine Solving Constrained. Non-linear Programming Problems, *Annals of Operations Research*, 5, 485-500, **1985**, in <http://www.mathworks.com>.
- [23] **Biggs, M. C.:** Constrained Minimization Using Recursive Quadratic Programming, Towards Global Optimization. LCW Dixon and GP Szergo, eds North-Holland 341–349, in <http://www.mathworks.com>, **1975**.
- [24] **Han, S. P.:** A Globally Convergent Method for Nonlinear Programming, *Journal of Optimization Theory and Applications*, 22:297, **1977**, in <http://www.mathworks.com>.
- [25] **Powell, M. J. D.:** The Convergence of Variable Metric Methods for Nonlinearly Constrained Optimization Calculations, *Nonlinear Programming 3*, OL Mangasarian, RR Meyer and SM Robinson, eds, Academic Press, in <http://www.mathworks.com>, **1978**.
- [26] **Powell, M. J. D.:** A Fast Algorithm for Nonlinearly Constrained Optimization Calculations, Numerical Analysis, GA Watson ed, *Lecture Notes in Mathematics*, Springer Verlag, 630, in <http://www.mathworks.com>, **1978**.
- [27] **Fletcher, R.:** Practical Methods of Optimization, John Wiley and Sons, in <http://www.mathworks.com>, **1987**.
- [28] **Gill, P. E., Murray, W. and Wright, M. H.:** Practical Optimization, London, Academic Press, in <http://www.mathworks.com>, **1981**.
- [29] **Powell, M.J.D.:** Variable Metric Methods for Constrained Optimization. Mathematical Programming: The State of the Art, A Bachem, M Grottschel and B Korte, eds Springer Verlag, 288–311, in <http://www.mathworks.com>, **1983**.
- [30] **Hock, W., Schittkowski, K. A.:** Comparative Performance Evaluation of 27 *Non-linear Programming Codes*, *Computing* 30:335, in <http://www.mathworks.com> **1983**.
- [31] <http://www.mathworks.com/help/optim/ug/constrained-nonlinear-optimization-algorithms.html>. Accessed **11 March 2016**.
- [32] <http://www.mathworks.com/help/optim/ug/fmincon.html>. Accessed **2016**.
- [33] http://www.mathworks.com/help/optim/ug/optimization-theory-overview.html#bqa_jby. Accessed **2016**.
- [34] **Silva, H.M., De Meireles, J.F.:** Effective Mechanical Behavior of Sandwich Beams under Uncoupled Bending and Torsion Loadings, *Applied Mechanics and Materials*, 590, 58–62, **2014**.
- [35] **Silva, H. M., De Meireles, J. F.:** Effective Stiffness Behavior of Sandwich Beams under Uncoupled Bending and Torsion Loadings, 852, b, 469–475, **2016**.

